

Improvement of Small Vessel Visibility in MIP Angiograms of TOF-MRA

E. G. Kholmovski¹, P. Vemuri^{1,2}, D. L. Parker¹

¹UCAIR, Department of Radiology, University of Utah, Salt Lake City, Utah, United States, ²Department of Electrical and Computer Engineering, University of Utah, Salt Lake City, Utah, United States

Introduction

The maximum intensity projection (MIP) algorithm [1] has been commonly used to simplify the analysis of volumetric MR angiography (MRA) studies due to its simplicity, robustness, and computational efficiency. One of the main drawbacks of the algorithm is a decrease in the visibility of small vascular structures in the resulting MIP images in comparison with the original cross-sectional images. The main reasons for this effect are a low contrast-to-noise ratio (CNR) between the small vessels and background tissues and variations in the background tissue intensity. These variations can be caused by non-ideal or ramped RF excitation pulses and/or spatially variable coil sensitivities. Improved MIP images can be generated if the intensity inhomogeneity of the background is removed. In this study, we have considered two techniques to improve small vessel visibility in MIP images constructed from 3D time-of-flight (TOF) MRA datasets with spatially varying background tissue intensity.

Theory and Methods

A median filter is well known for its ability to remove small structures with distinctive intensity from a constant or slowly varying background. The application of median filtering to black blood MRA was proposed in [2]. It was shown that the filter allows the construction of good quality minimum intensity projection (MinIP) angiograms of small vessels without prior segmentation of skull and surrounding air spaces. However, the improvement in small vessel visibility was accompanied by a loss and/or a distortion in large vascular structures. In this study, we consider the application of median filtering to white blood MRA to remove variations in background tissue intensity, so that the resulting MIP images have an improved visibility of small vessels without any loss of large vascular structure details.

Two approaches have been considered. In the first one, the image volume to be processed by the MIP algorithm is constructed as follows:

$$I_p(r) = I_o(r) - \alpha M\{I_o(r)\}$$

where $I_o(r)$ is the original image volume, $M\{\}$ denotes a median filtering operator, α ($\alpha \in [0, 1]$) is a parameter regulating the contributions of the original and median filtered image volumes to the resulting image volume $I_p(r)$. When $\alpha = 0$, the processed image volume is equivalent to the original one. The method proposed in [2] is analogous to our technique with $\alpha = 1$.

In the second technique, the image volume to be processed by the MIP algorithm is constructed as follows:

$$I_p(r) = I_o(r) - M\{S\{I_o(r)\}\}$$

where $S\{\}$ denotes the intensity thresholding operator. This operator is used to identify and remove intensity outliers from the image volume. In the case of TOF-MRA, any voxel with intensity significantly higher than the mean intensity of the voxel neighborhood can be considered as an outlier. The main purpose of the operator is to make the intensity of large vascular structures comparable to the intensity of the surrounding background tissue before application of the median filtering operation. The intensity thresholding operation can be implemented by subdividing the image volume into number of subvolumes, calculating mean and standard deviation of tissue voxels contained in each subvolume, and restricting voxel intensity in each subvolume to be less than or equal to the mean plus three the standard deviations for the given subvolume.

To test the proposed techniques, intracranial MRA studies were performed on a 3T Trio MR system (Siemens Medical Solutions, Erlangen, Germany) using a 3D TOF pulse sequence with flow compensation in the frequency and slice-selective directions. Imaging parameters: FOV=230x153.3 mm, in-plane matrix = 384x256, one axial 72-slice slab with 0.6 mm slice thickness, TR/TE=35/4.2 ms, 100 Hz/pixel bandwidth, a ramped RF pulse with an average flip angle of 20°. The eight-channel head coil (MRI Devices, Waukesha, WI) was used for the imaging studies. The data was zero-filled interpolated to achieve 0.3 mm isotropic voxel spacing and the eight edge slices on either end of the image slab were discarded. Median filtering was realized by subsequently applying a 1D median filter in three orthogonal directions. For the given image resolution, the filter kernel sizes were chosen to be 17, 17, and 11 elements in the x, y, and z directions, respectively.

Results

The typical MIP images calculated from the original and processed image volumes are shown in Fig. 1. The visibility of small vessels improves with an increase in the parameter α value. However, this improvement is accompanied by distortion in the appearance of large vascular structures (carotid siphon, middle cerebral arteries, and so on) for α close to 1 (Fig. 1d). The MIP image generated using the second technique has high visibility of small vessels similar to the visibility achieved by the first method with $\alpha=1$ but without any distortion in large vascular structures.

Discussion

Two techniques to improve small vessel visibility in MIP images constructed from TOF-MRA datasets have been considered. Both give a significant improvement in vessel visibility due to the suppression of background tissue intensity inhomogeneity. The quality of MIP images reconstructed from the image volume processed by the first technique crucially depends on the choice of the value of the parameter α . For the studied MRA datasets, it was found that $\alpha=0.5$ gives a substantial improvement in small vessels visibility without any noticeable loss in large vascular structures details. The second technique is more advantageous than the first one due to the absence of any parameters to adjust but it requires an additional step to remove intensity outliers.

Acknowledgments

This study was supported in part by NIH R01 HL48223 and Siemens Medical Solutions.

References

[1] Laub G. MRM 1990;14:222-229. [2] Alexander AL et al, MRM 2000;43:310-313.

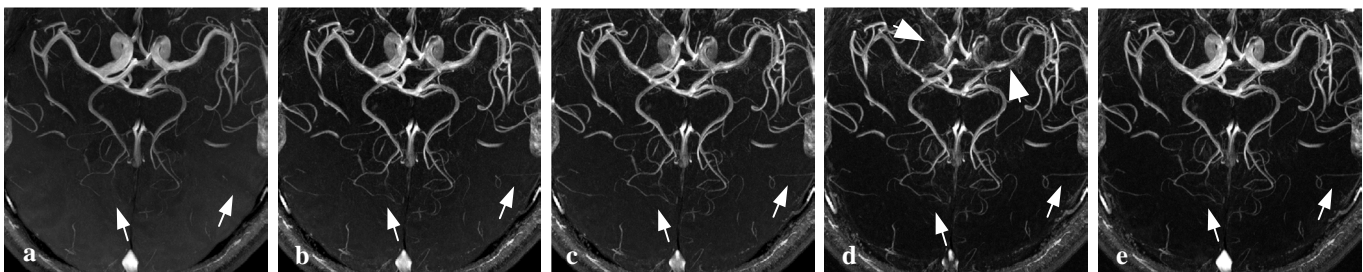


Figure 1. The MIP images constructed from the image volume processed by the first method with (a) $\alpha=0$ (the original image volume), (b) $\alpha=0.5$, (c) $\alpha=0.667$, and (d) $\alpha=1$. The MIP image shown in (e) was calculated from the image volume processed by the second technique. Wide arrows indicate the distortions in large vessels for $\alpha=1$. Narrow arrows show examples of the vascular structures that are not detectable in the MIP of the original dataset but easily identifiable in the MIP of the processed datasets.